DEUTSCHES ELEKTRONEN – SYNCHROTRON

DESY 91-004
February 1991

Characteristics of Leptonic Signals for Z Boson Pairs at Hadron Colliders

T. Matsura
II. Institut für Theoretische Physik, Universität Hamburg

J.J. van der Bij
Institute for Theoretical Physics, University of Amsterdam

ISSN 0418-9833

NOTKESTRASSE 85 · D-2000 HAMBURG 52

To be sure that your preprints are promptly included in the HIGH ENERGY PHYSICS INDEX, send them to the following (if possible by air mail):

DESY
Bibliothek
Notkestrasse 85
D-2000 Hamburg 52
Germany

DESY 91–004
February 1991

ISSN 0418–9833

Characteristics of leptonic signals for Z boson pairs at hadron colliders

T. Matsuura*
II. Institut für Theoretische Physik,
Universität Hamburg, D-2000 Hamburg 50

J.J. van der Bij†
Inst. voor Theor. Fysica, Univ. van Amsterdam
Amsterdam, the Netherlands

We study the production of Z boson pairs at hadron colliders followed by their subsequent decay into muons or electrons. We take into account the processes $q\bar{q} \to ZZ$ and $gg \to ZZ$. The calculation incorporates all effects of the polarization of the Z bosons. Particular emphasis is put on the Higgs-signal where we study the angular distribution of the decay leptons, in order to determine the longitudinal polarisation fraction of the Z bosons. We also study the correlation of the decay planes of the leptons from the two Z bosons. This correlation may be significant for light Higgs bosons.

*Supported by LAA, CERN, Geneva.
†KNAW-fellow

1 Introduction

Although the standard $SU(2)_L \times U(1)_Y$ electroweak gauge theory successfully explains all current data, certain parts of the theory have not been tested experimentally. The most important part of these is the mechanism of spontaneous symmetry breaking. Since in the standard model spontaneous symmetry breaking is due to the Higgs sector, the search for a Higgs particle is one of the main tasks for future colliders.

At present LEP100 gives a lower limit of about 41 GeV [1] for the Higgs boson mass. This limit can be improved to about 80 GeV at LEP200 [2]. For larger values of m_H one has to consider high energy hadron colliders such as the LHC (pp collisions at $\sqrt{s} = 16$ TeV) or the SSC (pp collisions at $\sqrt{s} = 40$ TeV). With the present lower limit on $m_t > 89$ GeV [3] a Higgs lying below the WW threshold will mainly decay into a $b\bar{b}$ pair. In this case there is an overwhelming direct QCD background, which dominates the signal. In this mass region the Higgs is therefore very difficult to find, even though one could try to use some rare decays as a signal. Rare decays already considered in the literature include, for example, $H \to \tau^+\tau^-$ [4-7], $H \to \gamma\gamma$ [4-11], $H \to Z\gamma$ [6,7,12], $H \to ZZ^*$ [6,7,13,14] or $H \to WW^*$ [6,13-15]. All of these signals are rather difficult to see [7]. The situation is much better for heavy Higgs bosons ($m_H > 2m_W$). For such a Higgs the main decay products are vector boson pairs, W^+W^- or ZZ [16]. A clear signal for the Higgs then consists of a peak in the invariant mass spectrum of the produced vector bosons. The double leptonic decay of the Z boson, $H \to ZZ \to l^+l^-l^+l^-$, leads to a particularly clean signal [17].

For a heavy top quark the largest production cross section for a Higgs boson is the gluon fusion process [18-20], except for the very largest Higgs masses ($m_H \gtrsim 600$ GeV), where vector boson fusion [21-23] becomes important. In this paper we will only be concerned with the gluon fusion process. For the top mass we take $m_t = 150$ GeV throughout the paper. The main background to detecting a heavy Higgs in the ZZ decay mode at hadron machines is the continuum production of Z boson pairs. The sources of continuum vector boson pairs are $q\bar{q}$ annihilation [24], gluon fusion[19,20] and vector boson fusion. As for the Higgs signal we ignore vector boson fusion here.

Higgs production through gluon-gluon fusion and its corresponding background, taking into account both $q\bar{q}$ annihilation and gluon fusion, have been studied before in [19,20]. It is the purpose of this paper to extend these studies by incoporating the decay of the Z bosons into leptons. All polarization effects of the Z bosons are kept. We therefore can make an analysis of angular distributions of the decay leptons. There are two distributions that we study. One is the distribution of the cosine of the polar angle, $\cos\theta$, of the decay leptons relative to the Z boson. Because the Higgs decays mainly into longitudinally polarized vector bosons the cross section $d\sigma/d\cos\theta$ should show a peaking near zero [23,25,26]. The other is the distribution of the angle ϕ between the decay planes of the two Z bosons. This distribution depends on the details of the Higgs production and decay mechanism. Within

the standard model a behaviour roughly like $1 + a\ \cos(2\phi)$ is expected [23,26,27], where the coefficient a can be sizeable for relatively small Higgs masses. For these distributions it is important to see what the effects of the lepton cuts are, because these cuts themselves can generate correlations among the outgoing leptons.

The paper is organized as follows. In section 2 we discuss the general characteristics of the signal and the background at the LHC and the SSC. In section 3 the $\cos\theta$ distribution and the decay plane correlation are discussed.

2 Cross sections

In this section we discuss the cross sections for Z boson pair production at the LHC and the SSC. We keep both the production by initial quarks as well as by incoming gluons. For the gluonic production of Z bosons we use the results of [20]. We remark that the amplitudes containing longitudinal polarizations in this paper should be multiplied by a factor -1. This change has no effect on integrated total cross sections, but does influence angular correlations. The decay of the Z bosons into leptons has been incorporated using the density matrix formalism. Furthermore, the propagators of the Z bosons have been treated in the narrow width approximation.

For the incoming partons we use the Duke and Owens structure functions [28] with $\Lambda = 0.2$ GeV evolved to a scale $Q^2 = \hat{s}/4$ and $\alpha_s = 12\pi/(23\ \log(Q^2/\Lambda^2))$. For the top quark mass we take everywhere $m_t = 150$ GeV. The various cross sections are obtained by means of a Monte Carlo integration over phase space and structure functions. In this integration cuts are imposed on the outgoing leptons. In order to crudely simulate a detector acceptance we take a rapidity cut of $|y_l| < 3$ and demand a transverse momentum $p_{Tl} > 20$ GeV for each lepton. The results we show are always for four outgoing muons and should be multiplied by a factor four if one wants to consider also outgoing electrons.

The total cross sections for two Z bosons decaying into muons with the above cuts are given in table 1 for a number of Higgs masses. We see that a sizeable number of events will be present both at the LHC and the SSC. In order to determine the mass of the Higgs boson the invariant mass spectrum of the Z boson pairs is needed. This is given in figs. 1 and 2 for the LHC and the SSC. The effect of the broadening of the Higgs peak for an increasing Higgs mass is clearly seen in these figures.

Another way to look for the Higgs is the study of the p_T spectrum of the outgoing Z bosons. Since the background is peaked at low transverse momentum, while the Higgs boson decays isotropically in its centre of mass frame, one expects a Jacobian peak above the background at

$$p_{TZ} = \frac{m_H}{2}\sqrt{1 - \frac{4m_Z^2}{m_H^2}} \tag{2.1}$$

This peak is indeed seen in figs. 3 and 4. The effect is more pronounced for heavier Higgs bosons. This suggests that one can improve the Higgs signal by

imposing a cut on the outgoing Z bosons of

$$p_{TZ} > \frac{m_{ZZ}}{4}\sqrt{1-\frac{4m_Z^2}{m_{ZZ}^2}} \tag{2.2}$$

This formula is a refinement of a previous suggestion $p_{TZ} > m_{ZZ}/4$, taking threshold effects into acccount. The effect of this cut can be seen in table 2, where we give the signal and background for a number of Higgs masses. The signal is defined by the total number of events in an invariant mass range $|m_{ZZ} - m_H| < \max(\Gamma_H, 10\text{ GeV})$. The background is defined as the number of events in the same range, but for $m_H = \infty$. We see that this cut improves somewhat the signal to background ratio, in particular for large Higgs masses.

3 Angular distributions

To obtain additional information on the Higgs we have also studied the angular distributions of the leptons. As far as we know it is the first time that both the $q\bar{q}$ and gg backgrounds have been considered in such a study. In the following we will restrict the invariant mass of the Z boson pair to the range $|m_{ZZ} - m_H| < \max(\Gamma_H, 10\text{ GeV})$.

The processes we are looking at are all of the type

$$X \to Z_1 Z_2 \to l_1\bar{l}_1 l_2\bar{l}_2 \tag{3.1}$$

where X is either the Higgs or one of the background processes. The decay angles θ_i and ϕ_i are defined as follows. Choose in the restframe of X the z-axis along the direction of motion of the vector boson Z_1. Now boost along the z-direction into the restframe of Z_1. In this frame the angles θ_1 and ϕ_1 are the polar and azimuthal angles of the lepton l_1. Repeating the above procedure for the other Z boson the angles θ_2 and ϕ_2 are found. The angles of interest are $\theta = \theta_1 = \theta_2$ (the θ_1 and θ_2 distributions are identical) and $\phi = \phi_1 + \phi_2$. The last one, ϕ, is the angle between the decay planes of the two Z bosons in the restframe of X.

The decay products of a heavy Higgs particle are predominantly longitudinally polarized Z bosons. Therefore, the angular distribution of the leptons in the Z rest frame is of the form,

$$\frac{d\sigma}{d\cos\theta} \sim \sin^2\theta \tag{3.2}$$

The background Z bosons, however, are mainly transversely polarized. This gives rise to the following $\cos(\theta)$ distribution

$$\frac{d\sigma}{d\cos\theta} \sim 1 + \cos^2\theta \tag{3.3}$$

One can therefore use this distribution in order to confirm that the signal is indeed the Standard Model Higgs. Explicit distributions are given in figs. 5 and 6.

For this distribution we have not applied the p_{TZ} cut of formula (2.2). One notices that for a relatively light Higgs the correlation is not very strong. This is because the coupling of the longitudinal vector bosons is proportional with the Higgs mass. Naively one therefore expects the correlation to grow with the Higgs mass. In the figures one sees however, that the effect is stronger for $m_H = 400$ GeV than for $m_H = 600$ GeV. The reason for this is that the signal to background ratio is worse for the heavier Higgs.

To show that the Higgs signal is responsible for the particular form of the $\cos(\theta)$-distribution, we have plotted in fig. 7 the same distribution for the background only ($m_H = \infty$) at the LHC energy. Here one recognizes the $1 + \cos^2(\theta)$ form, which corresponds to transversely polarized Z bosons, although it is somewhat distorted due to the lepton cuts.

We also made a comparison of the $q\bar{q}$-background distribution with the literature and find reasonable agreement with [17], which appears to differ from [29].

Before presenting the Monte Carlo results for the decay plane correlations, we will first give some analytical expressions for this distribution. If no cuts are imposed on the final state leptons the ϕ distribution can be calculated rather straigthforwardly using the density matrix formalism [27]. Using the parametrization for the polarization vectors given in eq. (3.2) of ref. [20], one finds

$$\begin{aligned}
\frac{d\hat{\sigma}}{d\phi} &= N \left\{ \frac{64}{9}(c_V^2 + c_A^2)^2 \sum_{a,b} \rho_{ab}^{ab} \right. \\
&\quad + 4\pi^2 c_V^2 c_A^2 \cos\phi \ \mathrm{Re}(-\rho_{00}^{++} - \rho_{--}^{00} + \rho_{0-}^{+0} + \rho_{-0}^{0+}) \\
&\quad - 4\pi^2 c_V^2 c_A^2 \sin\phi \ \mathrm{Im}(-\rho_{00}^{++} - \rho_{--}^{00} + \rho_{0-}^{+0} + \rho_{-0}^{0+}) \\
&\quad + \frac{32}{9}(c_V^2 + c_A^2)^2 \cos(2\phi) \ \mathrm{Re}(\rho_{--}^{++}) \\
&\quad \left. - \frac{32}{9}(c_V^2 + c_A^2)^2 \sin(2\phi) \ \mathrm{Im}(\rho_{--}^{++}) \right\}
\end{aligned} \tag{3.4}$$

where N is a process dependent normalization factor and c_V and c_A are the vector and axial couplings of the leptons to the Z boson. They are given by

$$\begin{aligned}
c_V^2 &= \frac{\pi\alpha}{4\sin^2\theta_W \cos^2\theta_W}(1 - 4\sin^2\theta_W)^2 \\
c_A^2 &= \frac{\pi\alpha}{4\sin^2\theta_W \cos^2\theta_W}
\end{aligned} \tag{3.5}$$

The density matrix ρ is defined by

$$\rho_{cd}^{ab} = \sum_X M(X \to Z_1^a Z_2^b) M^\dagger(X \to Z_1^c Z_2^d) \tag{3.6}$$

here $M(X \to Z_1^a Z_2^b)$ is the amplitude for producing a Z boson pair with helicities a and b. Because for the processes we are studying we have to identify angles ϕ

and $-\phi$, all information about the coefficients of the sine parts in eq. (3.4) is lost. Furthermore, if one cannot distinguish leptons from anti-leptons also the angles $\pi \pm \phi$ are equivalent to ϕ, which implies that only the coefficient of the $\cos(2\phi)$ term can be determined. However, as the coefficient of the $\cos\phi$ is rather suppressed compared to that of the $\cos(2\phi)$ due to the smallness of the vector coupling c_V, it is unlikely that the $\cos\phi$ part can be measured even if one can distinguish particles from anti-particles.

In case of the Standard Model Higgs signal and the $q\bar{q}$ background we have calculated explictly the decay plane correlations. For the Higgs signal one finds [26,27]

$$\begin{aligned}\frac{d\hat{\sigma}}{d\phi} &= \frac{1}{1024}\frac{1}{(4\pi)^4}\frac{\alpha^2\alpha_s^2}{\sin^4\theta_W\cos^4\theta_W}\frac{1}{s}\sqrt{1-\frac{4m_Z^2}{s}} \\ &\quad \frac{m_Z^2}{\Gamma_Z^2}\frac{m_q^4}{\left(s-m_H^2\right)^2+m_H^2\Gamma_H^2}|1+(1-\lambda)F(\lambda)|^2 \\ &\quad \left\{\frac{64}{9}(c_V^2+c_A^2)^2\frac{(s-2m_Z^2)^2+8m_Z^4}{4m_Z^4}+4\pi^2c_A^2c_V^2\frac{s-2m_Z^2}{m_Z^2}\cos\phi\right. \\ &\quad \left.+\frac{32}{9}(c_V^2+c_A^2)^2\cos(2\phi)\right\} \qquad (3.7)\end{aligned}$$

with $\lambda = 4m_q^2/s$ and

$$F(\lambda) = \begin{cases} \left\{\arcsin\left(\sqrt{\frac{1}{\lambda}}\right)\right\}^2 & \text{if } \lambda > 1 \\ -\frac{1}{4}\left\{\log\left(\frac{1-\sqrt{1-\lambda}}{1+\sqrt{1+\lambda}}\right)+i\pi\right\}^2 & \text{if } 0 \le \lambda \le 1 \end{cases} \qquad (3.8)$$

For the $q\bar{q}$ background we obtain

$$\begin{aligned}\frac{d\hat{\sigma}}{d\phi} &= \frac{1}{1536}\frac{1}{(4\pi)^4}(g_L^4+g_R^4)\frac{1}{s}\sqrt{1-\frac{4m_Z^2}{s}}\frac{m_Z^2}{\Gamma_Z^2}\int_{-1}^{1}d\cos\psi \\ &\quad \left\{\frac{64}{9}(c_V^2+c_A^2)^2A+4\pi^2c_A^2c_V^2B\cos\phi \qquad (3.9)\right. \\ &\quad \left.+\frac{32}{9}(c_V^2+c_A^2)^2C\cos(2\phi)\right\} \qquad (3.10)\end{aligned}$$

where ψ is the polar angle of the Z bosons in the C.M. frame of the incoming gluons. The left and right handed couplings of the quarks to the Z bosons, g_L and g_R, are equal to

$$g_L^2 = \begin{cases} \frac{16}{9}\pi\alpha\tan^2\theta_W & \text{for the u-type quarks} \\ \frac{4}{9}\pi\alpha\tan^2\theta_W & \text{for the d-type quarks} \end{cases} \qquad (3.11)$$

$$g_R^2 = \begin{cases} \frac{\pi\alpha}{\sin^2\theta_W\cos^2\theta_W}\left(1-\frac{4}{3}\sin^2\theta_W\right)^2 & \text{for the u-type quarks} \\ \frac{\pi\alpha}{\sin^2\theta_W\cos^2\theta_W}\left(1-\frac{2}{3}\sin^2\theta_W\right)^2 & \text{for the d-type quarks} \end{cases} \qquad (3.12)$$

The coefficients A, B and C in eq. (3.10) are given by

$$A = \frac{t}{u} + \frac{u}{t} + 4\frac{sm_Z^2}{ut} - 4m_Z^2\left(\frac{1}{t^2} + \frac{1}{u^2}\right) \tag{3.13}$$

$$B = -\frac{m_Z^2}{(s-4m_Z^2)^2}\left\{m_Z^2(sm_Z^2 + 4ut - 8m_Z^4)\left[\frac{1}{t} - \frac{1}{u}\right]^2 + s\left[m_Z^2\left(\frac{1}{t} + \frac{1}{u}\right) + 2\right]^2\right\} \tag{3.14}$$

$$C = \frac{m_Z^4(ut - m_Z^4)}{(s-4m_Z^2)^2}\left[\frac{1}{t} - \frac{1}{u}\right]^2 \tag{3.15}$$

The symbols s, t and u in the above equations are the usual Mandelstam variables. The hadronic cross sections can be obtained by folding eqs. (3.7) and (3.10) with the gg and $q\bar{q}$ fluxes, respectively.

From eq. (3.7) one can see that the correlation is only sizeable for a relatively light Higgs. This can also be seen in fig. 8 where we show for the LHC the decay plane correlation due to the Higgs signal only, for m_H =200, 400 and 600 GeV. For the SSC we find exactly the same results. We have checked that our MC program reproduces the results for the Higgs signal and the $q\bar{q}$ background as found by our analytical calculation.

For a more realistic study of the decay plane correlation we have imposed the same lepton cuts as mentioned before. Moreover, in our Monte Carlo also the gg background process, for which we have not calculated analytically the ϕ distribution, is taken into account. In figs. 9 and 10 we show the decay plane correlation after imposing the lepton cuts for three values of the Higgs mass. From these figures one can see that for a Higgs of 200 GeV the decay plane correlation might be observable. However, for a much heavier Higgs it does not seem probable that the correlation can be observed experimentally. To investigate the effects of the lepton cuts on the ϕ-distribution we have plotted in figs. 11 and 12 the decay plane correlation at the LHC, with and without the lepton cuts for a 200 GeV Higgs. As can be seen in fig. 11, without the lepton cuts the background is only very weakly correlated and it is the Higgs which is responsible for the correlation. However, after imposing the lepton cuts also the background gets correlated. We have found similar results for the SSC. As the lepton cuts clearly have the tendency to enhance the decay plane correlation for both signal and background, it is not clear whether this distribution can be used to distinguish a Standard Model Higgs from non-standard ones as suggested by [26,27].

Acknowledgements:
T. Matsuura thanks the University of Amsterdam and NIKHEF-H for their hospitality. The research of Dr. van der Bij has been supported by a fellowship of the Royal Netherlands Academy of Arts and Sciences.

References

1. ALEPH Collaboration, Phys. Lett. **B246**, (1990) 306.

2. See *e.g.* S. L. Wu *et al.* in *Proceedings of the ECFA Workshop on LEP200*, Volume II, Aachen, Germany, CERN report CERN 87-08, and references therein.

3. CDF Collaboration, preprint FERMILAB-Conf-90/138-E (1990).

4. I. Hinchliffe, in *Proceedings of the XXIII International Conference on High Energy Physics*, Berkeley, California, 1986, edited by S. Loken, (World Scientific, Singapore, 1987), p. 1264

5. R. K. Ellis, I. Hinchliffe, M. Soldate and J. J. van der Bij, Nucl. Phys. **B297**, (1988) 221.

6. J. F. Gunion, P. Kalyniak, M. Soldate and P. Galison, Phys. Rev. **D34**, (1986) 101.

7. J. F. Gunion, G. L. Kane and J. Wudka, Nucl. Phys. **B299**, (1988) 231.

8. J. Ellis, M. K. Gaillard and D. V. Nanopoulos, Nucl. Phys. **B106**, (1976) 292.

9. J. P. Leveille, Phys. Lett. **B83**, (1979) 123.

10. A. I. Vainshtein, M. B. Voloshin, V. I. Zakharov and M. A. Shifman, Sov. J. Nucl. Phys. **30**, (1979) 711.

11. D. A. Dicus and S. S. D. Willenbrock, Phys. Rev. **D37**, (1988) 1801.

12. R. Cahn, M. S. Chanowitz and N. Fleishon, Phys. Lett. **B82**, (1979) 113.

13. T. G. Rizzo, Phys. Rev. **D22**, (1980) 722.

14. W.-Y. Keung and W. J. Marciano, Phys. Rev. **D30**, (1984) 248.

15. E. W. N. Glover, J. Ohnemus and S. S. D. Willenbrock, Phys. Rev. **D37**, (1988) 3193.

16. B. W. Lee, C. Quigg and H. Thacker, Phys. Rev. **D16**, (1977) 1519.

17. V. Barger, T. Han and R. J. N. Phillips, Phys. Lett. **B206**, (1988) 339.

18. H. M. Georgi, S. L. Glashow, M. E. Machacek and D. V. Nanopoulos, Phys. Rev. Lett. **40** , (1978) 692.

19. D. A. Dicus, C. Kao and W. W. Repko, Phys. Rev. **D36**, (1987) 1570.

20. E. W. N. Glover and J. J. van der Bij, Phys. Lett. **B219**, (1989) 488 and Nucl. Phys. **B321**, (1989) 561.

21. R. N. Cahn and S. Dawson, Phys. Lett. **B136**, (1984) 196, Erratum: **B138**, (1984) 464;
S. Dawson, Nucl. Phys. **B249**, (1984) 42;
G. L. Kane, W. W. Repko and W. B. Rolnick, Phys. Lett. **B148**, (1984) 367.

22. M. S. Chanowitz and M. K. Gaillard, Phys.Lett. **B142**, (1984) 85.

23. A. Abbasabadi and W. W. Repko, Nucl. Phys. **B292**, (1987) 461 and Phys. Rev. **D37**, (1988) 2668.

24. R. W. Brown and K. O. Mikaelian, Phys. Rev. **D19**, (1979) 922.

25. M. J. Duncan, Phys. Lett. **B179**, (1986) 393.

26. M. J. Duncan, G. L. Kane and W. W. Repko, Phys. Rev. Lett. **55**, (1985) 773 and Nucl. Phys. **B272**, (1986) 517.

27. J. R. Dell'Aquila and C. A. Nelson, Phys. Rev. **D33**, (1986) 80;
C. A. Nelson, Phys. Rev. **D37**, (1988) 1220.

28. D. W. Duke and J. F. Owens, Phys. Rev. **D30**, (1984) 49.

29. H.-U. Bengtsson and A. Savoy-Navarro, Phys. Rev. **D37**, (1988) 1787.

Tables

Table 1

Total cross sections for ZZ production, followed by $Z \to \mu^+\mu^-$. Muon cuts of $|y_l| < 3$ and $p_{Tl} > 20$ GeV are assumed.

$\sigma(fb)$	$m_H = 200$ GeV	$m_H = 400$ GeV	$m_H = 600$ GeV	$m_H = \infty$
LHC (16 TeV)	9.7	8.8	7.3	6.7
SSC (40 TeV)	28.1	26.7	20.1	17.3

Table 2

Signal and background for the Higgs. The signal is defined as the cross section after imposing the following cuts: $|m_{ZZ} - m_H| < \max(\Gamma_H, 10 \text{ GeV})$, $|y_l| < 3$ and $p_{Tl} > 20$ GeV. The background as the cross section with the same cuts, but for $m_H = \infty$. The background is given between brackets.

$\sigma(fb)$	$m_H = 200$ GeV	$m_H = 400$ GeV	$m_H = 600$ GeV
LHC (no cut)	4.49 (1.43)	1.91 (0.33)	0.70 (0.29)
LHC (p_T cut)	3.84 (1.16)	1.62 (0.19)	0.55 (0.17)
SSC (no cut)	14.7 (3.45)	8.13 (0.91)	3.16 (0.90)
SSC (p_T cut)	12.7 (2.80)	7.17 (0.56)	2.68 (0.57)

Figure Captions

1. Invariant mass distribution for Z boson pairs at the LHC.
2. Invariant mass distribution for Z boson pairs at the SSC.
3. Transverse momentum distribution of the Z bosons at the LHC.
4. Transverse momentum distribution of the Z bosons at the SSC.
5. Distribution of the lepton decay angle θ in the Z rest frame at the LHC.
6. Distribution of the lepton decay angle θ in the Z rest frame at the SSC.
7. Distribution of the lepton decay angle θ in the Z rest frame at the LHC for only the background.
8. Decay plane correlation of the Z bosons from the Higgs signal without cuts at the LHC.
9. Decay plane correlation of the Z bosons from the Higgs signal + background, including lepton cuts, at the LHC.
10. Decay plane correlation of the Z bosons from the Higgs signal + background, including lepton cuts, at the SSC.
11. Decay plane correlation of the Z bosons for a 200 GeV Higgs, without lepton cuts, at the LHC.
12. Decay plane correlation of the Z bosons for a 200 GeV Higgs, including lepton cuts, at the LHC.

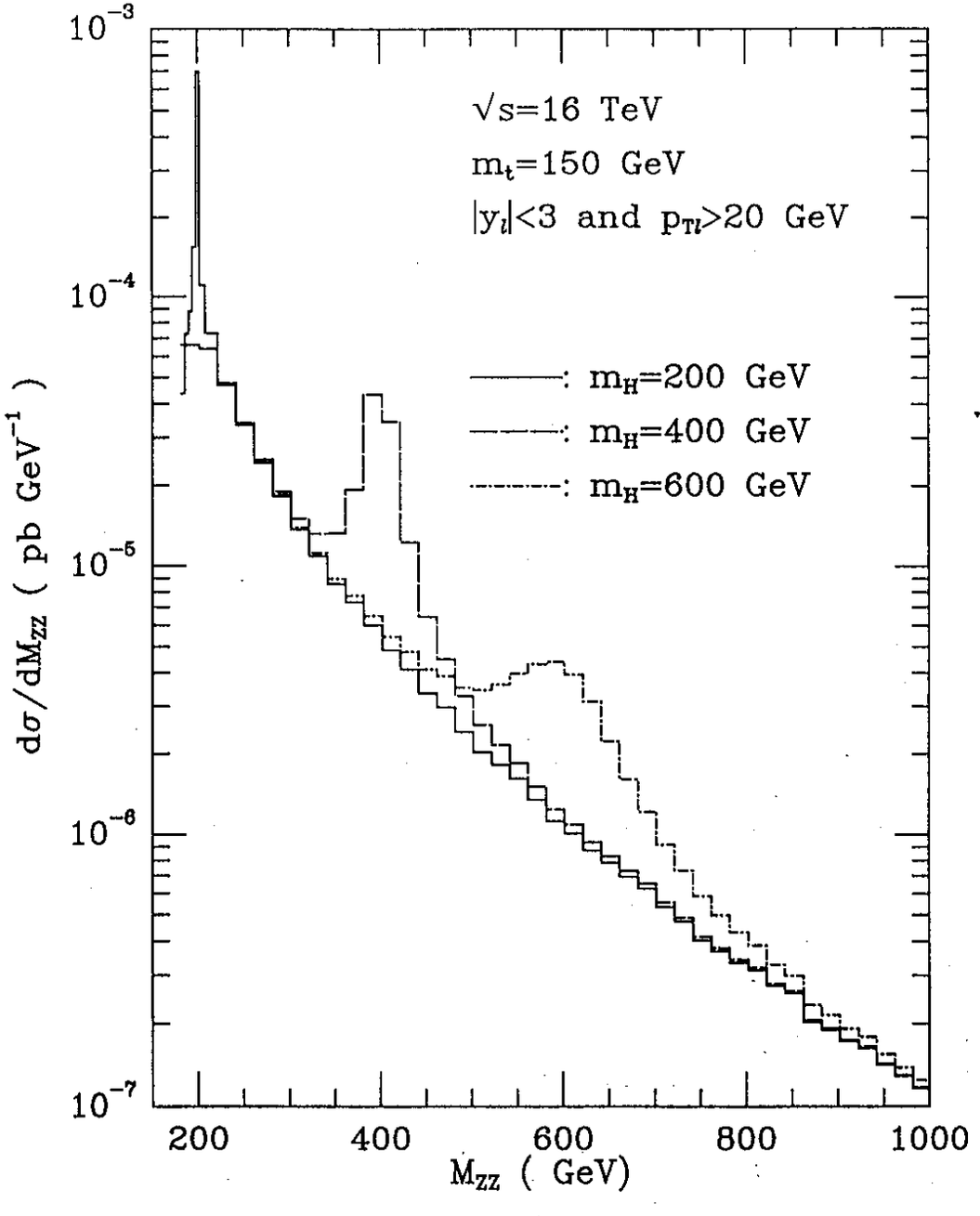
√s=16 TeV
m_t=150 GeV
$|y_l|$<3 and p_{Tl}>20 GeV
: m_H=200 GeV
: m_H=400 GeV
: m_H=600 GeV
$d\sigma/dM_{ZZ}$ (pb GeV^{-1})
M_{ZZ} (GeV)

Fig. 1

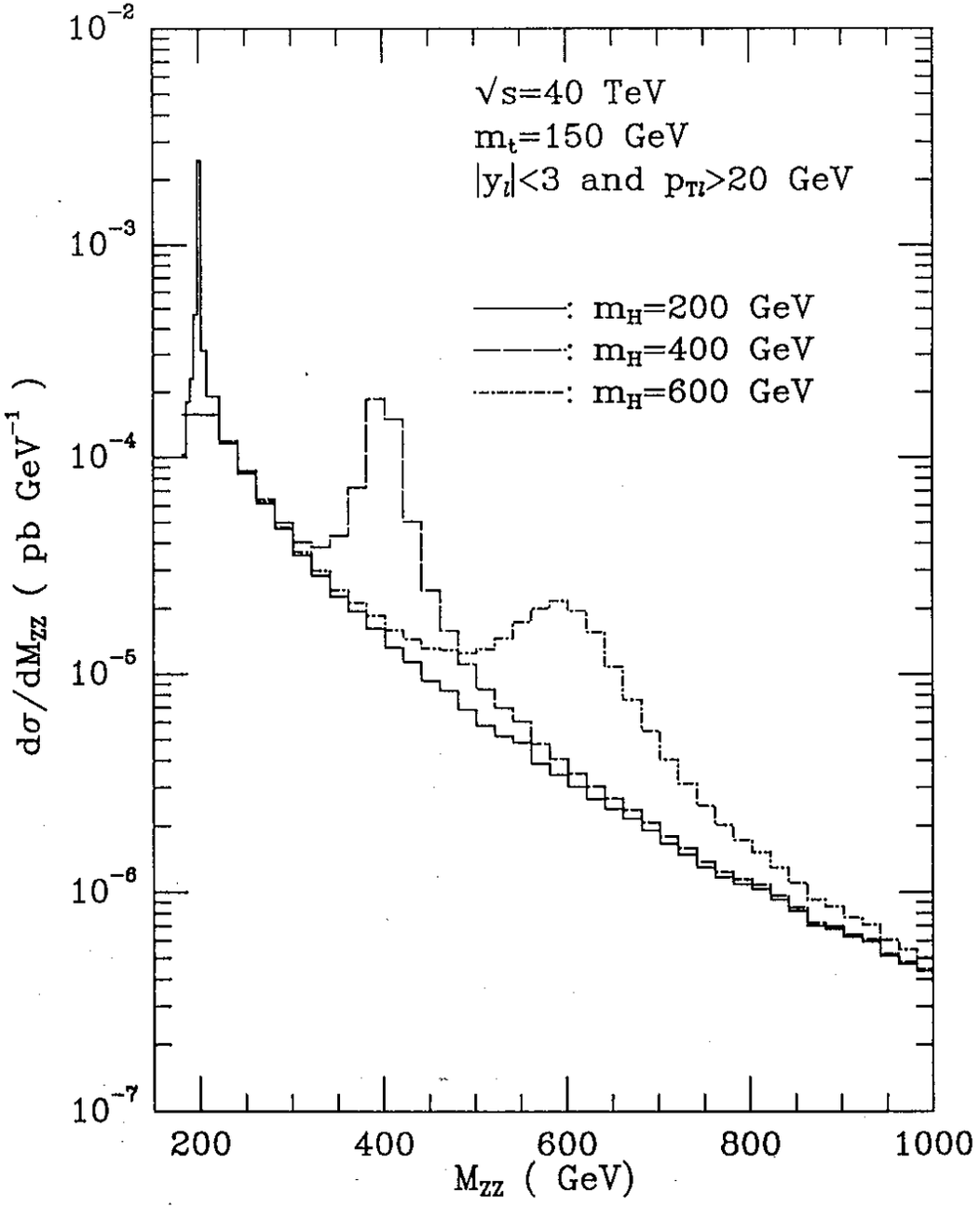
√s=40 TeV
m_t=150 GeV
$|y_l|$<3 and p_{Tl}>20 GeV
: m_H=200 GeV
: m_H=400 GeV
: m_H=600 GeV
$d\sigma/dM_{ZZ}$ (pb GeV^{-1})
M_{ZZ} (GeV)

Fig. 2

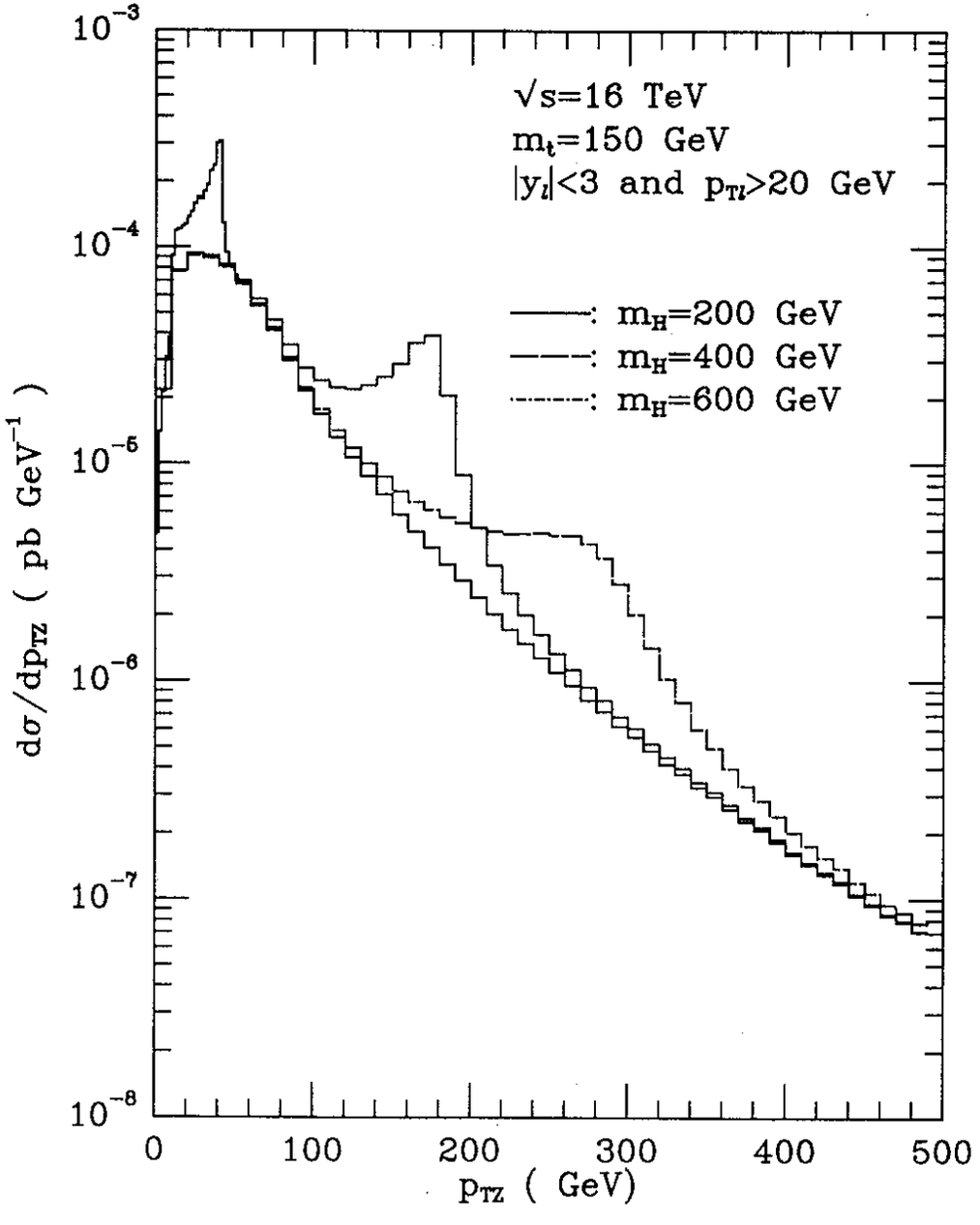
√s=16 TeV
m_t=150 GeV
$|y_l|$<3 and p_{Tl}>20 GeV
: m_H=200 GeV
: m_H=400 GeV
: m_H=600 GeV
$d\sigma/dp_{TZ}$ (pb GeV^{-1})
p_{TZ} (GeV)

Fig. 3

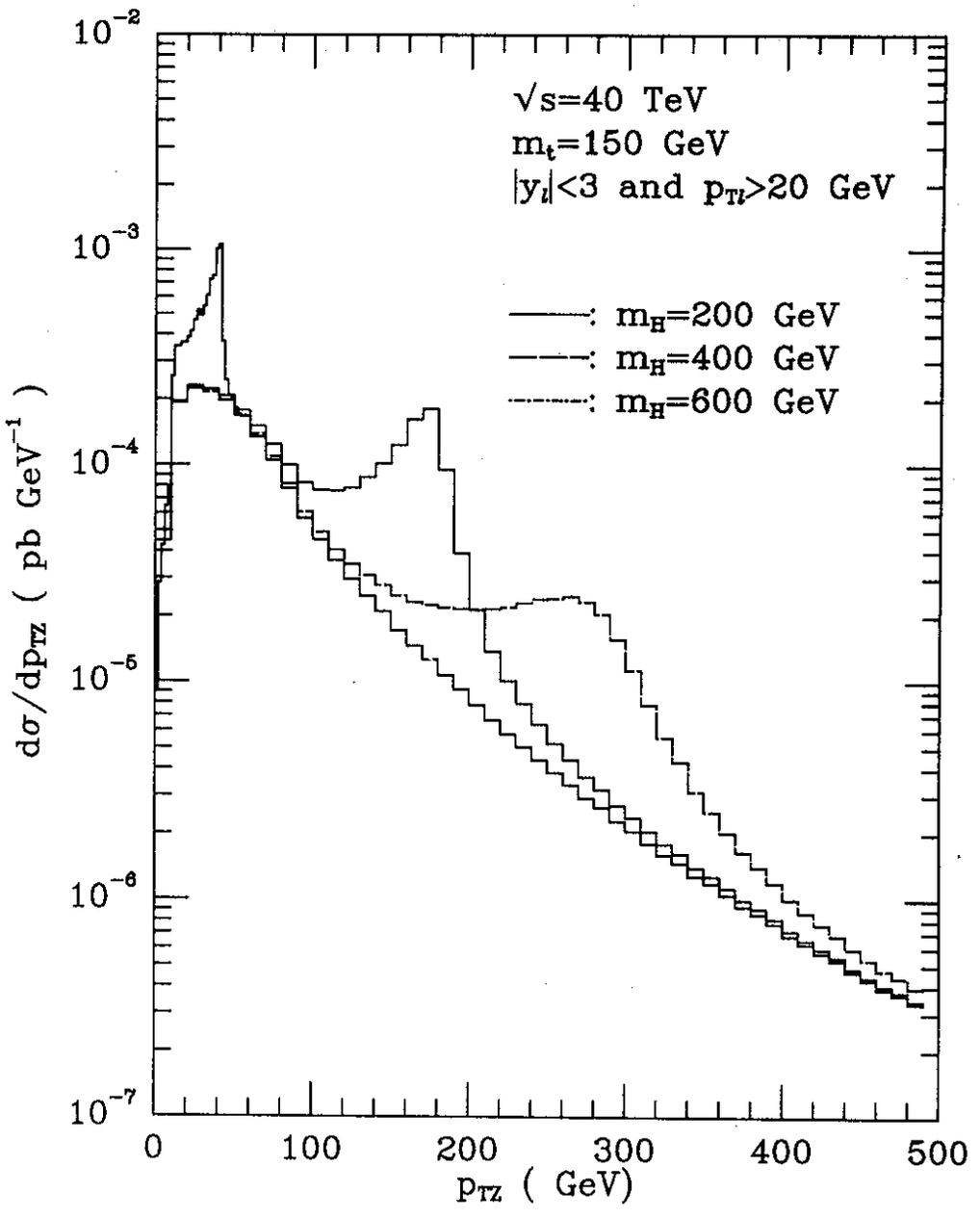
√s=40 TeV
m_t=150 GeV
$|y_l|$<3 and p_{Tl}>20 GeV
: m_H=200 GeV
: m_H=400 GeV
: m_H=600 GeV
$d\sigma/dp_{TZ}$ (pb GeV^{-1})
p_{TZ} (GeV)

Fig. 4

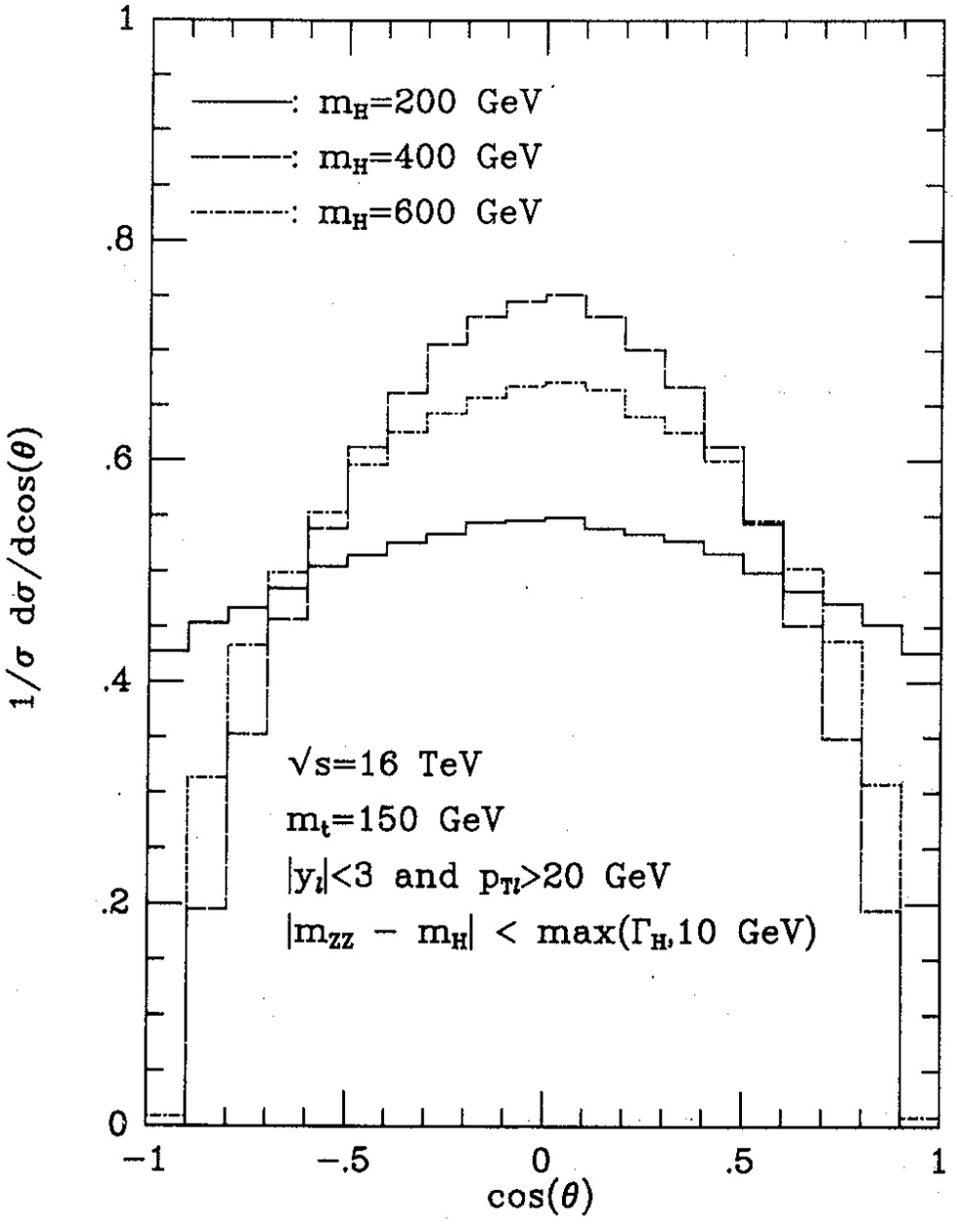
: m_H=200 GeV
: m_H=400 GeV
: m_H=600 GeV
√s=16 TeV
m_t=150 GeV
$|y_l|$<3 and p_{Tl}>20 GeV
$|m_{ZZ} - m_H|$ < max(Γ_H,10 GeV)
$1/\sigma\ d\sigma/d\cos(\theta)$
$\cos(\theta)$
0
.2
.4
.6
.8
1
−1
−.5
0
.5
1

Fig. 5

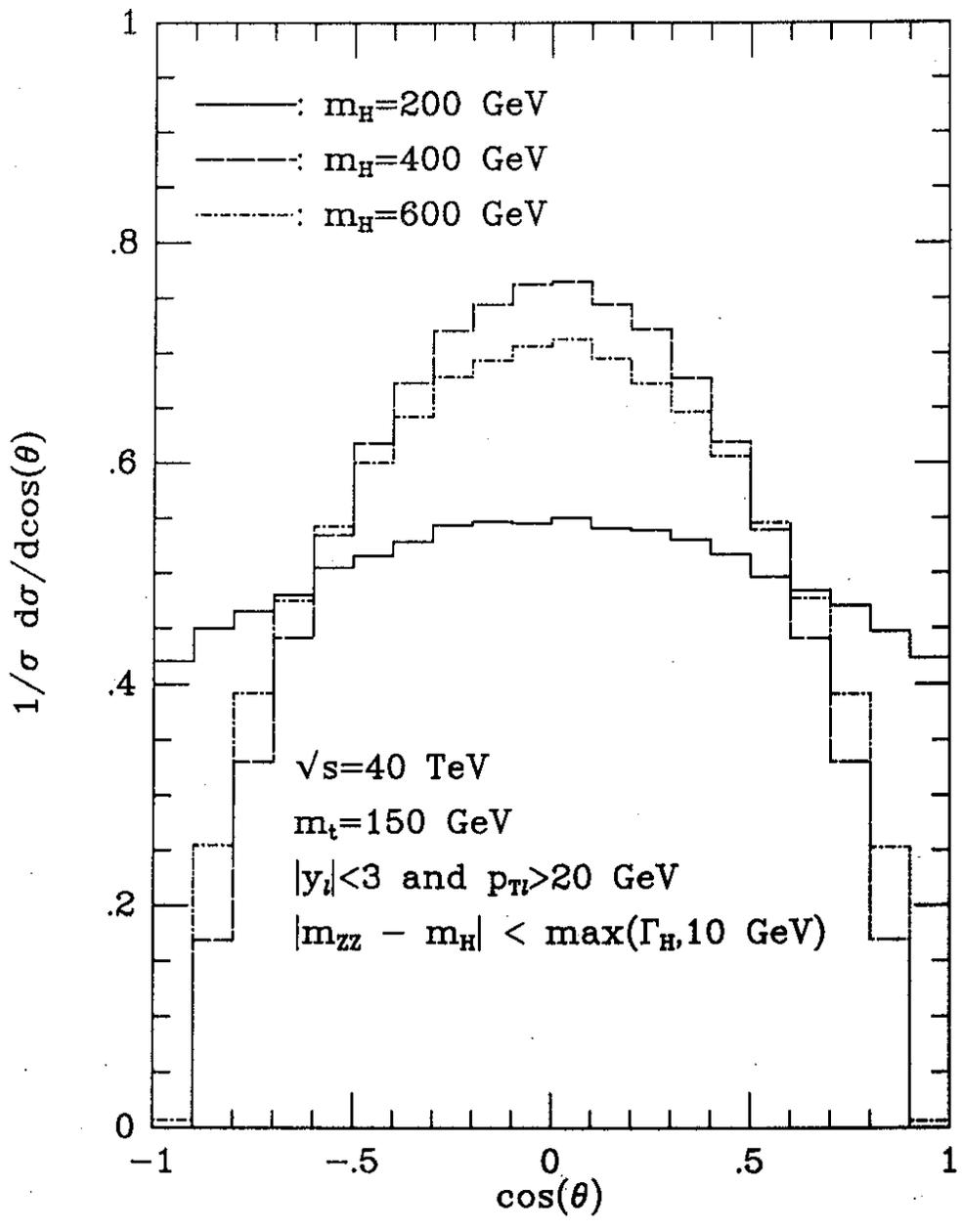
: m_H=200 GeV
: m_H=400 GeV
: m_H=600 GeV
√s=40 TeV
m_t=150 GeV
$|y_l|$<3 and p_{Tl}>20 GeV
$|m_{ZZ} - m_H|$ < max(Γ_H,10 GeV)
$1/\sigma\ d\sigma/d\cos(\theta)$
$\cos(\theta)$
0
.2
.4
.6
.8
1
−1
−.5
0
.5
1

Fig. 6

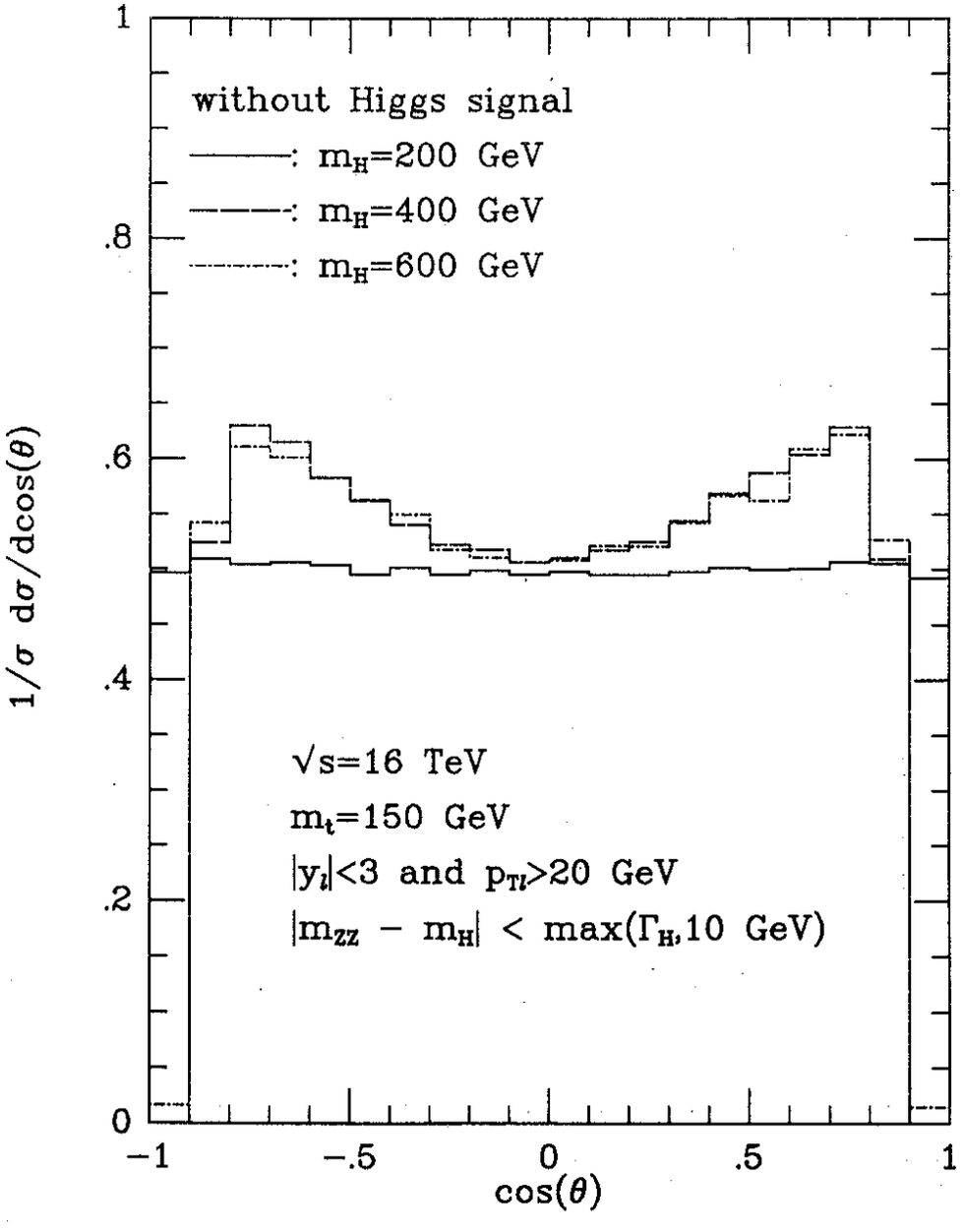
without Higgs signal
——: m_H=200 GeV
– – –: m_H=400 GeV
–·–·–: m_H=600 GeV
√s=16 TeV
m_t=150 GeV
$|y_l|$<3 and p_{Tl}>20 GeV
$|m_{ZZ} - m_H| < \max(\Gamma_H, 10\ \text{GeV})$
$1/\sigma\ d\sigma/d\cos(\theta)$
$\cos(\theta)$
1
.8
.6
.4
.2
0
−1
−.5
0
.5
1

Fig. 7

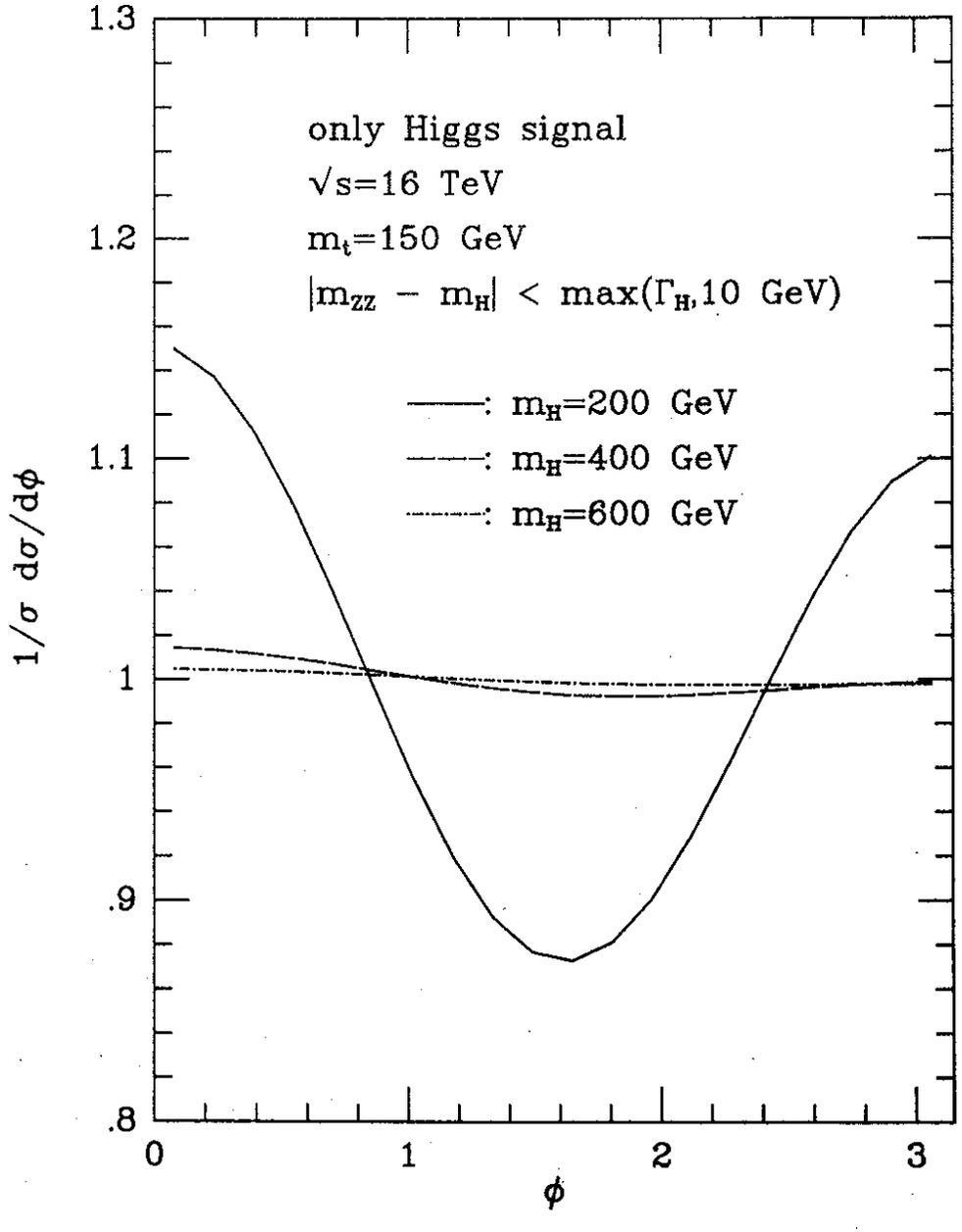
only Higgs signal
√s=16 TeV
m_t=150 GeV
$|m_{ZZ} - m_H| < \max(\Gamma_H, 10\ \text{GeV})$
——: m_H=200 GeV
– – –: m_H=400 GeV
–·–·–: m_H=600 GeV
$1/\sigma\ d\sigma/d\phi$
ϕ
1.3
1.2
1.1
1
.9
.8
0
1
2
3

Fig. 8

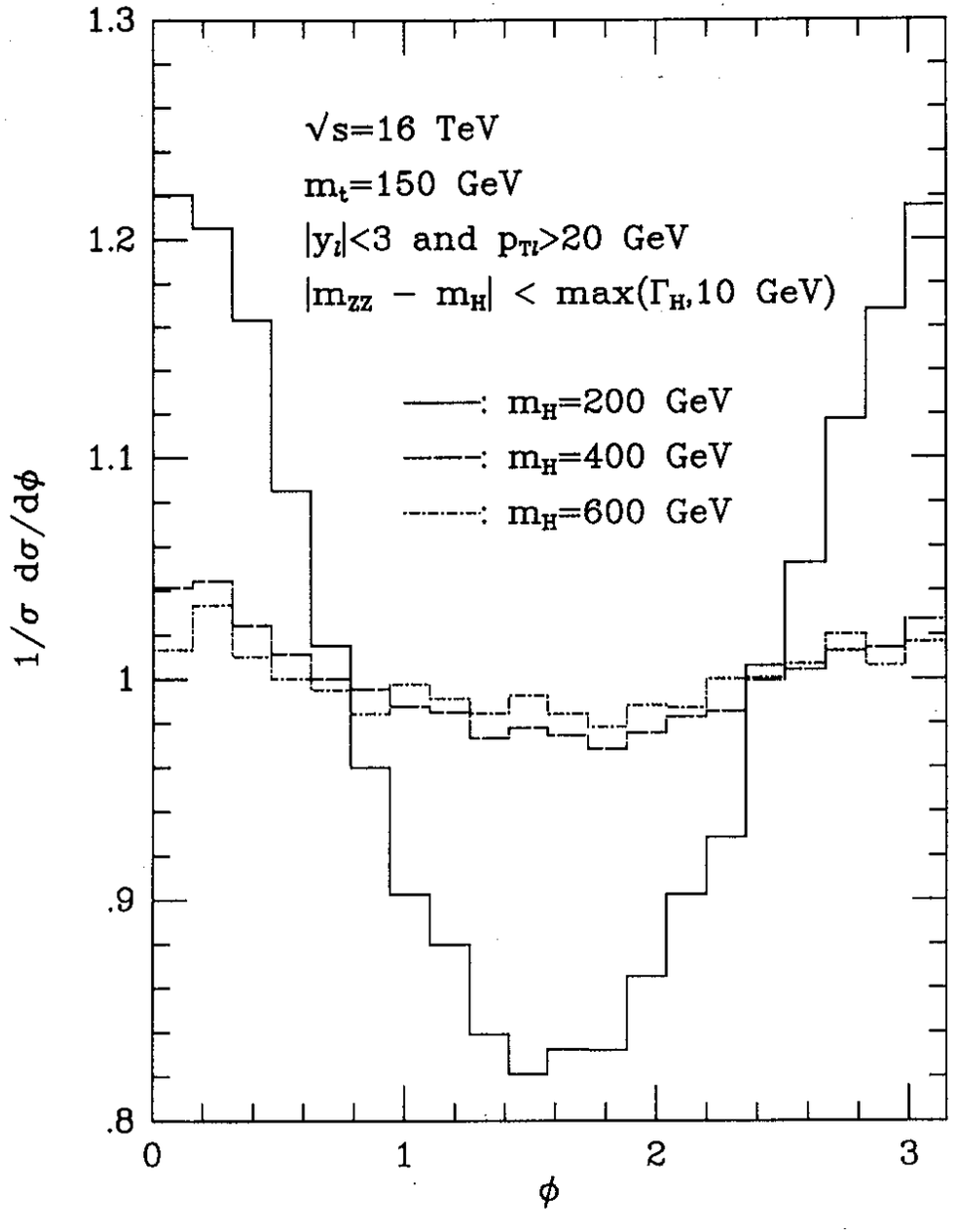
√s=16 TeV
m_t=150 GeV
$|y_l|$<3 and p_{Tl}>20 GeV
$|m_{ZZ} - m_H| < \max(\Gamma_H, 10\ \text{GeV})$
——: m_H=200 GeV
——: m_H=400 GeV
——: m_H=600 GeV
$1/\sigma\ d\sigma/d\phi$
ϕ
1.3
1.2
1.1
1
.9
.8
0
1
2
3

Fig. 9

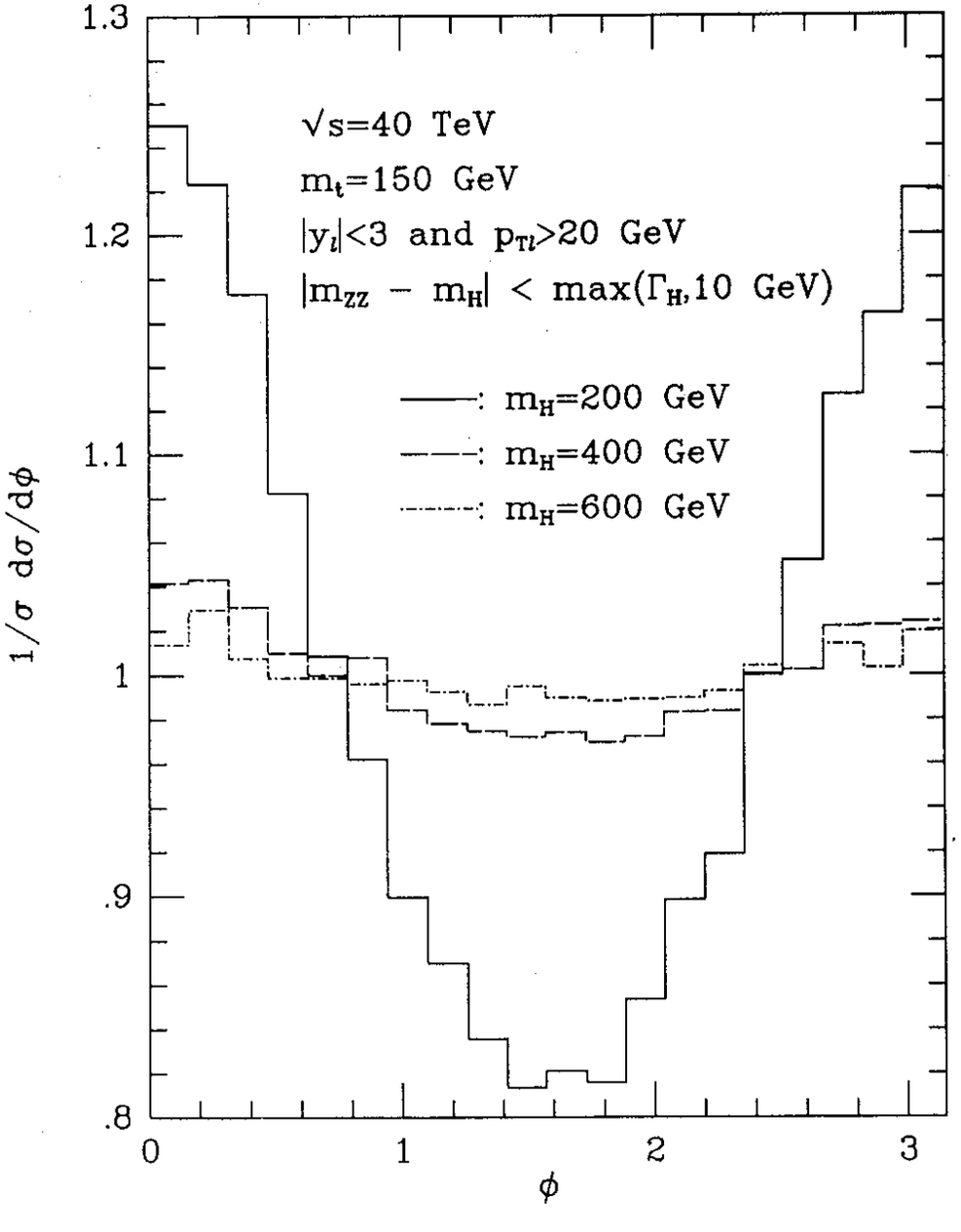
√s=40 TeV
m_t=150 GeV
$|y_l|$<3 and p_{Tl}>20 GeV
$|m_{ZZ} - m_H| < \max(\Gamma_H, 10\ \text{GeV})$
——: m_H=200 GeV
——: m_H=400 GeV
——: m_H=600 GeV
$1/\sigma\ d\sigma/d\phi$
ϕ
1.3
1.2
1.1
1
.9
.8
0
1
2
3

Fig. 10

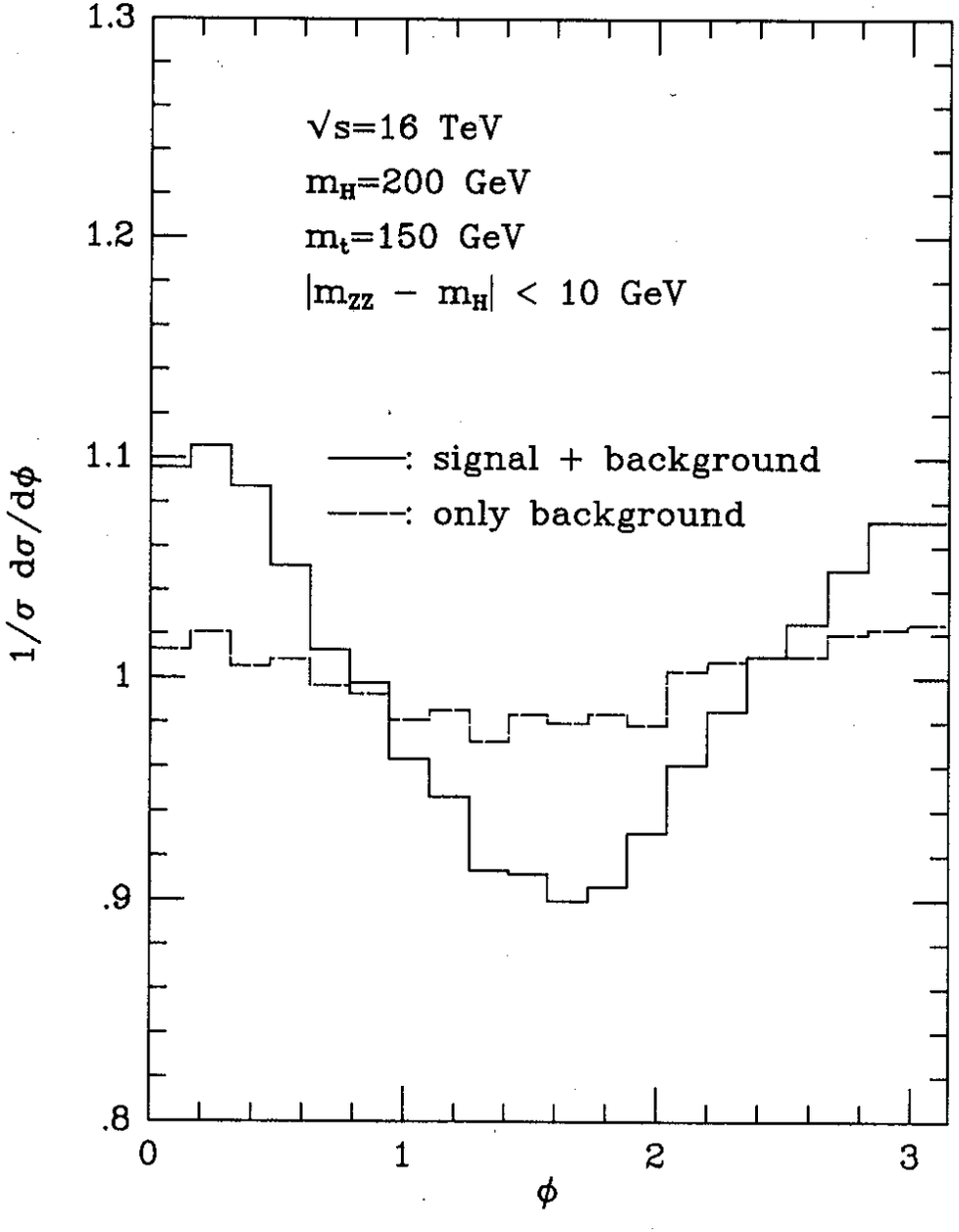
√s=16 TeV
m_H=200 GeV
m_t=150 GeV
$|m_{ZZ} - m_H| < 10$ GeV
——: signal + background
– – –: only background
$1/\sigma\ d\sigma/d\phi$
ϕ
1.3
1.2
1.1
1
.9
.8
0
1
2
3

Fig. 11

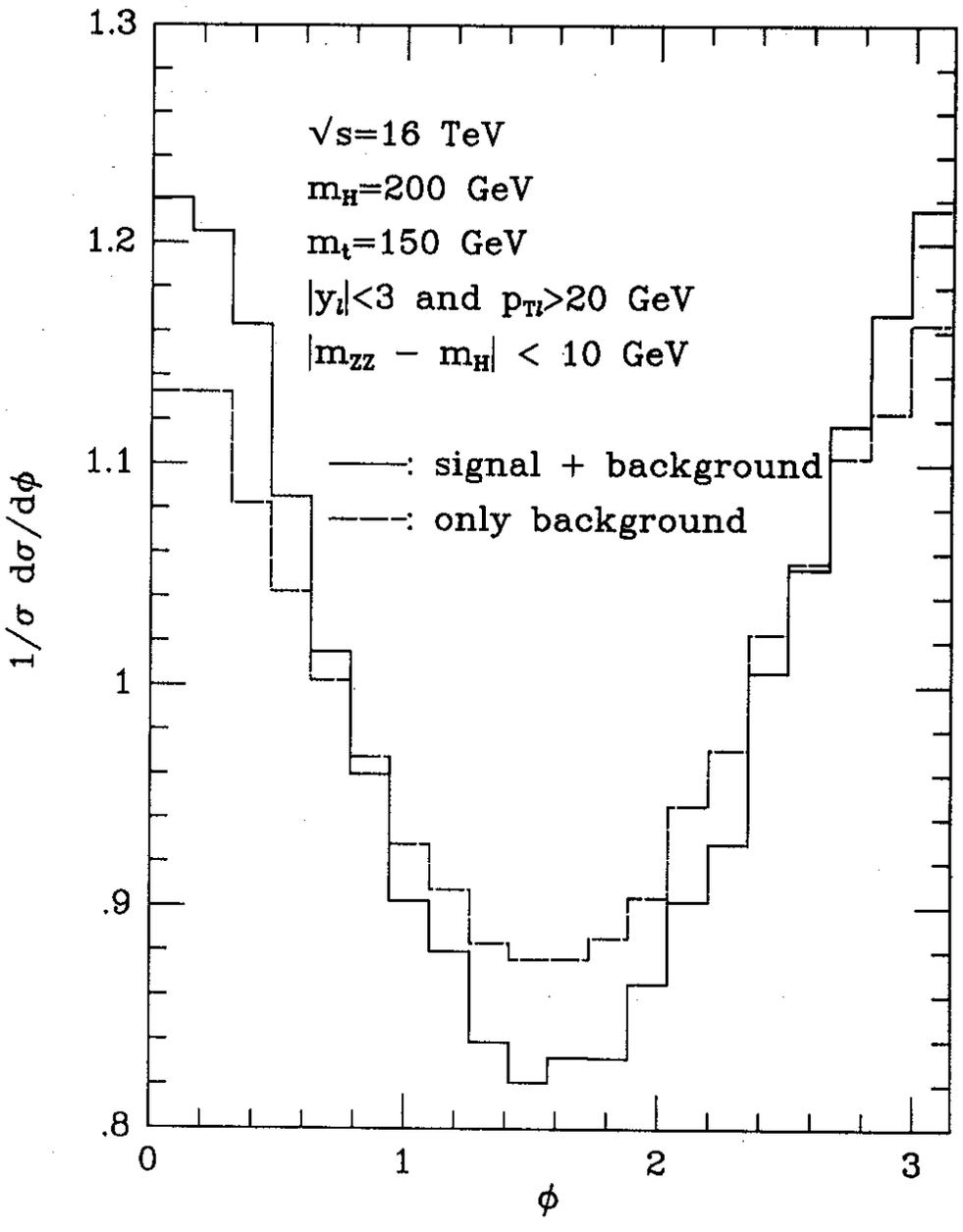
√s=16 TeV
m_H=200 GeV
m_t=150 GeV
$|y_l|<3$ and $p_{Tl}>20$ GeV
$|m_{ZZ} - m_H| < 10$ GeV
——: signal + background
– – –: only background
$1/\sigma\ d\sigma/d\phi$
ϕ
1.3
1.2
1.1
1
.9
.8
0
1
2
3

Fig. 12